

Temperature-Sensitive Micrometer-Thick Layers of Hyaluronan Grafted on Microspheres

Derk Joester,^{*,†} E. Klein,[‡] Benjamin Geiger,[§] and Lia Addadi[†]

Contribution from the Departments of Structural Biology and Molecular Cell Biology and Chemical Research Support, Weizmann Institute of Science, Rehovot, Israel

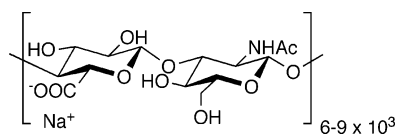
Received June 8, 2005; Revised Manuscript Received November 30, 2005; E-mail: derk.joester@weizmann.ac.il

Abstract: The giant polyelectrolyte glycosaminoglycan hyaluronan (1–10 MDa) is a major component of the pericellular coat on a variety of cells, where it is an important modulator and mediator of early cell adhesion events. This pericellular layer can reach 5 μm thickness on cells that produce cartilage (chondrocytes), and up to 2 μm on *Xenopus laevis* kidney epithelial cells (A6). We are interested in generating model systems for the pericellular coat in order to learn more about the structure and function of hyaluronan on biological or artificial surfaces. We report here the synthesis of model systems where a coat of coordinatively cross-linked hyaluronan of up to 2 μm thickness was covalently photografted onto polystyrene microspheres. The hydrated coat was imaged directly by environmental scanning electron microscopy (ESEM) at close to 100% relative humidity. The key feature of the procedure is the reversible reverse-temperature phase transition of hyaluronan induced by trivalent lanthanide cations, which is exploited to achieve sufficient density for grafting of thick layers. The microsphere-grafted coat shows a temperature-dependent swelling when labeled with lanthanide ions (Gd^{3+} or Tb^{3+}). We directly observed a volume contraction of 20% with increasing temperature between 1 and 11 $^{\circ}\text{C}$ by wet-mode ESEM.

Introduction

Hyaluronan (Chart 1) is an ultra-high molecular weight glycosaminoglycan ($M_w = 1\text{--}10$ MDa) that is responsible in part for the pressure stability of cartilage, is the key lubricant in joints, and plays an important role in cell adhesion and cancer metastasis.^{1–3} It is widely used to modulate surface properties in biomedical and biomaterials applications and especially in implant materials and devices. Hyaluronan-based hydrogels have found application—among others—in wound repair,⁴ in surface passivation and anti-fouling,³ and in tissue engineering.⁵ It is furthermore used as a visco-supplement in joints and in ophthalmic surgery.⁶ Hyaluronan recently emerged also as a mediator and modulator of early stages of cell adhesion.^{7,8} As such, it is capable of conveying highly specific chiral recognition of surfaces to the cell⁹ while its exceptionally strong binding

Chart 1. Structure of the Repeat Unit of the Glycosaminoglycan Hyaluronan, the Sodium Salt of Hyaluronic Acid^a



^a Alternating 1,3- β -N-acetylglucosamine (GlcNAc) and 1,4- β -glucuronic acid units form very long linear chains (DP > 2500, $M_w = 1\text{--}10$ MDa). The polyelectrolyte carries one carboxylate group per repeat unit. The charged groups are spaced by about 1 nm along the chain, and disaccharides are twisted by 180 $^{\circ}$ relative to each other, such that the carboxylates point in opposite directions.

to certain substrates can prevent the development of mature adhesions and induce apoptosis.¹⁰

The latter functions depend on the presence of hyaluronan in the pericellular coat, an extracellular membrane-anchored layer of polysaccharides, glycoproteins, and proteoglycans. Hyaluronan layers in the pericellular coat can reach a thickness of 2 μm in A6 epithelial cells and 5 μm in the case of chondrocytes, cells that produce hyaluronan in cartilage.⁷ This is orders of magnitude larger than expected from simple adlayers, where the thickness is determined by the radius of gyration, which is on the order of 100–200 nm, depending on the length of the polymer. A rare example of a well-characterized surface layer of fully hydrated hyaluronan was reported by Morra et al.¹¹ They created an overlayer of 100 nm thickness

[†] Department of Structural Biology;

[‡] Chemical Research Support.

[§] Department of Molecular Cell Biology.

- (1) Garg, H.; Hales, C. In *Chemistry and Biology of Hyaluronan*; Elsevier: New York, 2004, p 580.
- (2) Lapeik, L.; De Smedt, S.; Demeester, J.; Chabreck, P. *Chem. Rev.* **1998**, *98*, 2663–2684.
- (3) Morra, M. *Biomacromolecules* **2005**, *6*, 1205–1223.
- (4) Chen, W. Y. J.; Abatangelo, G. *Wound Repair Regen.* **1999**, *7*, 79–89.
- (5) (a) Mori, M.; Yamaguchi, M.; Sumitomo, S.; Takai, Y. *Acta Histochem. Cytochem.* **2004**, *37*, 1–5. (b) Lee, K. Y.; Mooney, D. J. *Chem. Rev.* **2001**, *101*, 1869–1879.
- (6) (a) Balazs, E.; Denlinger, J. In *The biology of hyaluronan*; Evered, D., Whelan, J., Eds.; J. Wiley & Sons: Chichester, U.K., 1989; pp 265–280; (b) Balazs, E.; Laurent, T. In *The chemistry, biology, and medical applications of hyaluronan and its derivatives*; Laurent, T., Ed.; Portland Press: London, 1998; pp 325–336.
- (7) Cohen, M.; Klein, E.; Geiger, B.; Addadi, L. *Biophys. J.* **2003**, *85*, 1996–2005.
- (8) Zimmerman, E.; Geiger, B.; Addadi, L. *Biophys. J.* **2002**, *82*, 1848–1857.
- (9) Hanein, D.; Geiger, B.; Addadi, L. *Science* **1994**, *263*, 1413–1416.

(10) Hanein, D.; Yarden, A.; Sabanay, H.; Addadi, L.; Geiger, B. *Cell Adhesion Commun.* **1996**, *4*, 341.

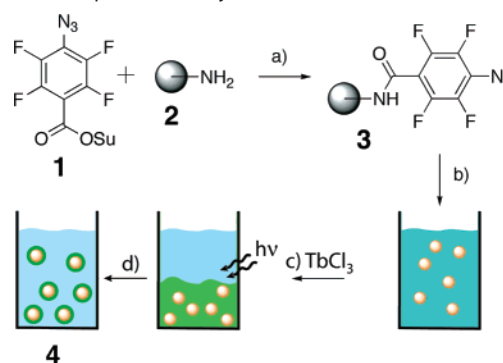
(11) Morra, M.; Cassinelli, C.; Pavesio, A.; Renier, D. *J. Colloid Interface Sci.* **2003**, *259*, 236–243.

by absorbing hyaluronan on a polyethylenimine- (PEI-) treated surface. This layer was found to be highly compressible by atomic force microscopy (AFM) in water. Covalent cross-linking of the two polyelectrolytes caused the layer to become thinner (40–50 nm) and stiffer. Sackmann and co-workers^{12,13} report hydrated hyaluronan layers of 50–250 nm that were prepared by immobilization of hyaluronan binding proteins. In contrast, Suh et al.¹⁴ report the dry thickness of a chemisorbed layer of hyaluronan on glass to be only 3 nm. This difference of more than one order of magnitude between the thicknesses of dry and hydrated layers is a manifestation of the swelling of hyaluronan in water. For a recent comprehensive review of the aspects of immobilizing hyaluronan on surfaces with an emphasis on different synthetic techniques, see Morra.³

To gain insight into the structure and function of the pericellular hyaluronan, a synthetic reference system would be advantageous. The currently available techniques do not, however, allow construction of layers of biological dimensions. Thick layers are frequently based on polyelectrolyte multilayers^{15,16} or covalent cross-linking of hyaluronan chains (e.g., see Barbucci and co-workers¹⁷). The latter approach would be feasible for the grafting of layers on beads. However, the covalent inter/intrachain cross-linking of hyaluronan does not reflect the situation in the cells, where the cross-links are formed by relatively weak interactions between polysaccharides and proteins. Furthermore, a significant increase in stiffness was observed in cross-linked hydrogels as opposed to non-cross-linked ones.¹⁵ We thus decided to work with functionalized surfaces and native hyaluronan rather than with functionalized hyaluronan to avoid random covalent cross-linking.

Prestwich and co-workers¹⁸ recently described the temperature-dependent solubility of mixtures of hyaluronan with trivalent lanthanide cations. At physiological pH, some 70%² of the carboxylic acid groups of the polyelectrolyte are dissociated and thus available to form complexes with the highly charged lanthanide cations. Monodentate binding of carboxylates to lanthanides is frequently entropy-driven and enthalpy-opposed, and leads to inner- and outer-sphere complexes.¹⁹ Multidentate binding, especially in the presence of nitrogen-containing ligands, gives rise to extremely stable ($pK_d > 22!$) inner-sphere complexes.²⁰ Contrary to the conventional behavior of organic salt complexes, the lanthanide–hyaluronan complex becomes less soluble with increasing temperature. When hyaluronan of a certain molecular weight is mixed with a lanthanide chloride at low temperature (1.5 °C), the complex is soluble. With increasing temperature, a phase transition occurs at a well-defined transition temperature, the lower critical solubility

Scheme 1. Preparation of Hyaluronan-Coated Beads^a



^a (a) PBS, RT, 16 h; (b) hyaluronan; (c) TbCl₃; (d) *hν*, RT → 60 °C, 15 min.

temperature (LCST²¹), at which the hyaluronan salt condenses and precipitates. This transition is immediately detectable by an increase in the turbidity of the sample. At the same time the volume of the hyaluronan phase contracts and water is expelled. The LCST for hyaluronan of a given molecular weight depends strongly on the nature of the lanthanide cation; for a given cation it decreases with increasing molecular weight of hyaluronan. It was shown that the transition for a Dy³⁺–hyaluronan complex is fully reversible, albeit with a significant amount of hysteresis. This LCST phase behavior was found to be specific for hyaluronan: chondroitin sulfates precipitate irreversibly, while heparin solutions remain homogeneous when lanthanide salts are added.

Here we show how the unusual phase behavior of hyaluronan in the presence of lanthanide cations can be exploited to graft micrometer-thick layers of hyaluronan onto polystyrene microspheres. We also characterize the thermal response of layers grafted in such fashion. This is the first report on grafting of hyaluronan layers of more than a few hundred nanometers thickness.

Results

Hyaluronan (1.6 MDa, 150 mmol/L NaCl, pH = 7.4) forms viscous aqueous solutions at low concentrations; chains start to overlap at 0.59 mg/mL and entangle above 2.4 mg/mL.²² Solutions of up to 10 mg/mL can be prepared but are difficult to handle because of the extreme viscosity. To avoid the necessity to stir, filter, or remove any kind of side product or reagent, a photo-cross-linking approach was selected for the grafting step.

Preparation of Beads. Active ester **1** was prepared according to literature (Scheme 1).²³ Amino-terminated polystyrene beads (**2**, i.d. = 5.8 μm; Polysciences, Inc.) were then coupled with **1** to give photo-cross-linker-modified beads **3**.

Grafting Attempt. Functionalized beads **3** (Scheme 1) were suspended in a hyaluronan solution (3 mg/mL, ca. 1 μmol/L) in water at 24 °C and irradiated. Irrespective of the molecular weight of the hyaluronan, this corresponds to a concentration

- (12) (a) Albersdorfer, A.; Sackmann, E. *Eur. Phys. J. B* **1999**, *10*, 663–672. (b) Sengupta, K.; Schilling, J.; Marx, S.; Markus, F.; Sackmann, E. *Biophys. J.* **2003**, *84*, 381A–381A.
- (13) Sengupta, E.; Schilling, J.; Marx, S.; Fischer, M.; Bacher, A.; Sackmann, E. *Langmuir* **2003**, *19*, 1775–1781.
- (14) Suh, K. Y.; Yang, J. M.; Khademhosseini, A.; Berry, D.; Tran, T. N. T.; Park, H.; Langer, R. J. *Biomed. Mater. Res., Part B* **2005**, *72B*, 292–298.
- (15) Richert, L.; Engler, A. J.; Discher, D. E.; Picart, C. *Biomacromolecules* **2004**, *5*, 1908–1916.
- (16) Picart, C.; Sengupta, K.; Schilling, J.; Maurstad, G.; Ladam, G.; Bausch, A. R.; Sackmann, E. *J. Phys. Chem. B* **2004**, *108*, 7196–7205.
- (17) (a) Pasqui, D.; Rossi, A.; Barbucci, R.; Lamponi, S.; Gerli, R.; Weber, E. *Lymphology* **2005**, *38*, 50–65. (b) Barbucci, R.; Magnani, A.; Lamponi, S.; Pasqui, D.; Bryan, S. *Biomaterials* **2003**, *24*, 915–926.
- (18) Vercruyse, K. P.; Li, H.; Luo, Y.; Prestwich, G. D. *Biomacromolecules* **2002**, *3*, 639–643.
- (19) Kim, Y. I.; Choi, S. N.; Song, C. G. *Bull. Korean Chem. Soc.* **2001**, *22*, 641–643.
- (20) Micskei, K.; Helm, L.; Brucher, E.; Merbach, A. E. *Inorg. Chem.* **1993**, *32*, 3844–3850.

- (21) Reverse temperature phase transitions at a lower critical solubility temperature have been most thoroughly investigated for N-substituted polyacrylamides. For a recent review on stimuli-responsive biopolymers, see Gil, E. S.; Hudson, S. A. *Prog. Polym. Sci.* **2004**, *29*, 1173–1222.
- (22) Krause, W. E.; Bellomo, E. G.; Colby, R. H. *Biomacromolecules* **2001**, *2*, 65–69.
- (23) (a) Yan, M. D.; Cai, S. X.; Wybourne, M. N.; Keana, J. F. W. *Bioconjugate Chem.* **1994**, *5*, 151–157. (b) Keana, J. F. W.; Cai, S. X. *J. Org. Chem.* **1990**, *55*, 3640–3647.

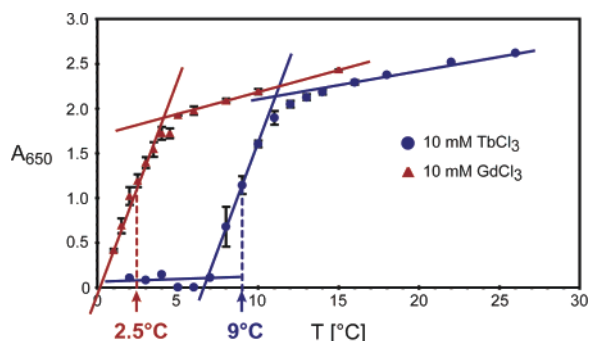


Figure 1. Reverse temperature phase transition at lower critical solubility temperature (LCST) of bulk hyaluronan (2.4–3.6 MDa), induced by Tb^{3+} (blue) and Gd^{3+} (red) ions, determined according to Prestwich et al.¹⁸ The phase transition at ambient pressure is indicated by the sharp increase in turbidity (A_{650}) with increasing temperature.

of 75 mmol/L in monomer units (i.e., the disaccharide sodium salt, $M_w = 400$ g/mol). After separation, the beads were imaged under wet conditions by ESEM (Figure 2A, see below). No hyaluronan coat could be detected. The failure of this initial attempt at grafting thick layers is most likely due to the fact that the concentration of hyaluronan in actual contact with the bead surface was too low. Because the mobility of entangled hyaluronan chains is much reduced, the very reactive nitrene generated from the photolinker azide on the surface of the bead under these conditions is mostly quenched by water.

To create much higher concentrations of hyaluronan on the surface of the beads for subsequent cross-linking, we decided to harness the reversible precipitation of hyaluronan in the presence of lanthanide cations.¹⁸

Phase Transition of Bulk Hyaluronan–Lanthanide Complexes. To characterize the behavior of the particular salt-free hyaluronan preparation (2.7 mg/mL, 2.4–3.6 MDa) we used for synthesis, we followed the reverse temperature phase transition in the presence of 10 mmol/L Gd^{3+} or Tb^{3+} as described by Prestwich and co-workers.¹⁸ Turbidity as an indicator for the phase transition was determined by reading the absorbance at $\lambda = 650$ nm (A_{650}) as a function of increasing temperature. The transition temperature, defined as the temperature of half-maximum change of A_{650} , is 2.5 °C for Gd^{3+} and 9 °C for Tb^{3+} (Figure 1). In our hands the temperature-dependent turbidity was fully reversible with very short equilibration times (seconds). The dense hyaluronan phase that formed above the transition temperature, however, did not revert to the original volume upon cooling. For weeks at 4 °C, the hyaluronan remained in a subvolume of the original solution, transparent but visually distinguishable from the excluded water. In the presence of 50–150 mmol/L NaCl and minor amounts of phosphate buffer, the precipitation of the same hyaluronan was dramatically slowed at room temperature and went to completion within seconds only upon heating to 60 °C. On the other hand, the transition was completely reversible relative to both turbidity and volume on cooling to 4 °C.

Grafting of Hyaluronan. The photolinker-functionalized beads **3** were suspended in a hyaluronan solution (final concentration = 2.7 mg/mL) in water at 24 °C. TbCl_3 was added at a final concentration of 10 mmol/L. The phase transition occurred within seconds. The majority of beads were trapped in a dense precipitate phase formed by the Tb^{3+} –hyaluronan complex. Cross-linking was then carried out by brief irradiation

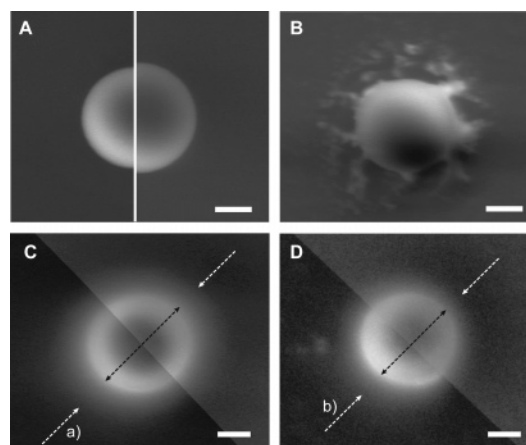


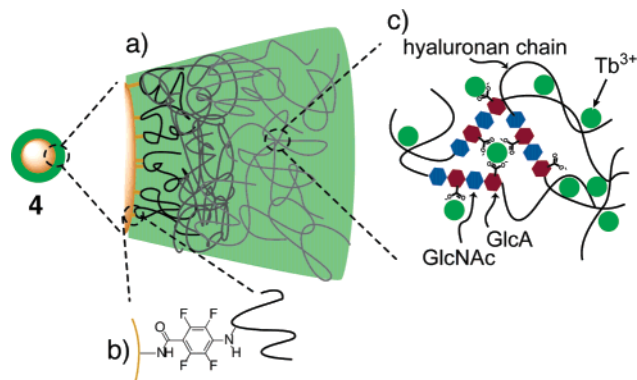
Figure 2. Wet-mode ESEM images. (A) Photo-cross-linking of hyaluronan from solution in the absence of lanthanide salt gives no detectable coat on photolinker-modified beads (right panel). No photodamage occurred to the bead. The bead appears identical to a bead that was precipitated with hyaluronan and Tb but not exposed to UV light (left panel). (B–D) Cross-linking was carried in the presence of Tb^{3+} . (B) Coated bead after forceful drying. Small amounts of fuzzy, still partially hydrated material are left after an almost explosive drying event. (C) Fully hydrated terbium–hyaluronan complex coats on polystyrene beads. The coat appears as a fuzzy “halo” around the bead. To compensate for detector asymmetry, the upper right and lower left parts of panels C and D were adjusted separately. (C) Fully expanded hyaluronan coat (1.9 μm) at 1 °C (4.7 Torr, 630 Pa). (D) Contracted coat (1.4 μm) at 11 °C (9.6 Torr, 1280 Pa). Scale bar = 2 μm .

with UV light. Subsequently, the suspension was cooled below the transition temperature and the coated beads **4** were separated by centrifugation. For all subsequent steps the coated beads were kept under water (pH = 5.8). After several rounds of washing in water at low temperature to remove excess salt and hyaluronan, the beads were imaged by wet-mode ESEM (see below). This washing procedure is bound to remove all water-suspended or loosely associated hyaluronan by shear and dilution. After this procedure, a coat of 1 μm or more was observed around most of the beads (Figure 2C,D). The coat was stable and unchanged for at least 3 days when the beads were kept suspended in water at 4 °C. In the presence of trivalent ions, the polystyrene microspheres are no longer colloidal stable and tend to aggregate. In contrast, the coated beads are not particularly prone to aggregation, which may be due to colloidal stabilization by the gel coat.

The hyaluronan associated with the beads at this stage likely is made from entangled and coordinatively cross-linked hyaluronan chains, some of which are directly and covalently connected to the polystyrene microsphere (Scheme 2). We do not know the counterion balance for the carboxylate groups of the hyaluronan in our preparations, that is, the ratio of $\text{Tb}^{3+}/\text{Na}^+/\text{H}^+$, and consequently have no way of knowing how much Tb is in the coat. However, we did not observe precipitation of excess salt upon evaporation of the bulk water in which samples were suspended. This is an indication that the bulk salt concentrations are low and consequently the complexes are quite stable.

If the irradiation step was omitted or irradiation was performed in the absence of terbium, no halos were observed (Figure 2A). Thus, condensation of the hyaluronan is necessary to achieve sufficient density for covalent grafting of hyaluronan to the surface of the bead. No photodamage to beads was observed under the conditions of irradiation used for grafting.

Scheme 2. Schematic Representation of the Gel Coat Grafted to Polystyrene Beads 4^a



^a (a) The layer of hyaluronan molecules closest to the bead surface is covalently bound to the bead, possibly with more than one bond. These bonds (b) are formed by insertion of highly reactive nitrene intermediates generated from the azide precursor **3** by UV irradiation. Chains further away from the surface are less likely connected covalently, but are entangled and coordinatively cross-linked through multiple Tb^{3+} ions (c).

Wet-Mode ESEM. Environmental scanning electron microscopy (ESEM) at water vapor pressures near the dew point [$p(\text{H}_2\text{O}) = 6.5$ Torr, 867 Pa, $T = 5$ °C] was recently shown to be an effective tool to observe the fully hydrated hyaluronan pericellular coat on cells in the presence of UO_2^{2+} , a contrast agent.⁷ Here we extended this technique to the Tb-labeled bead-grafted hyaluronan coat where Tb^{3+} takes on the role of UO_2^{2+} . Bulk water was slowly evaporated from the samples by drying under conditions of humidity close to the dew point. Samples emerged from bulk water and stayed hydrated at pressures below the dew point (90–100% relative humidity). The halos of hyaluronan-coated beads are characteristically fuzzy and semi-transparent to the electron beam. Shrinkage under the beam was minimal. The halos can only be dried down to leave a very small amount of solid residue at much lower relative humidity (Figure 2B). In contrast, droplets of water without any solute evaporate immediately under the same environmental conditions.

In a further extension of the technique, we performed wet-mode ESEM at variable temperatures to characterize the swelling behavior of the Tb-labeled hyaluronan coat as a

function of temperature. Samples were equilibrated for about an hour at a temperature below (1 °C) or above (11 °C) the transition temperature of bulk Tb–hyaluronan (9 °C). Vapor pressures were chosen to be closely below the dew point at the respective temperature. Images were taken and analyzed as described in the Supporting Information. To the best of our knowledge, this account is the first to show that wet-mode ESEM can be used to follow a temperature-dependent contraction in the fully hydrated state.

Temperature Response. Bulk hyaluronan undergoes a sharp phase transition and concomitant volume change at 9 °C in the presence of TbCl_3 (Figure 1). We observed a parallel temperature-dependent change of about 20% in the thickness of the fully hydrated gel coat grafted to the beads. Below the LCST, at 1 °C (4.6 Torr, 613 Pa), the expanded coat measures 1.9 ± 0.3 μm , while above the LCST, at 11 °C (9.6 Torr, 1280 Pa), it shrinks to 1.5 ± 0.2 μm (Figure 2C,D). This shrinkage is due to the phase transition and not to a general effect of increasing temperature because in that case expansion would ensue.

In bulk, the transition is fast and occurs on the order of seconds. On the beads, samples are equilibrated in the ESEM at the final temperature for at least 1 h, and the transition is complete in that time. The transition is thus too fast to be followed by this technique. There is no way to estimate the absolute concentration of hyaluronan in either the expanded or the contracted coat from the ESEM images alone. The relative change in concentration of hyaluronan, however, can be approximately evaluated: if beads and coats are perfectly spherical and homogeneous, that is, the hyaluronan concentration does not depend on the distance to the surface of the bead, then the shrinkage corresponds to an increase in concentration by 40%.

The coat thickness was determined from intensity profiles taken from digital images of coated beads. Typical intensity profiles of coated beads at 1 and 11 °C and in the absence of a coat are displayed in Figure 3A. Thickness distributions are narrow ($\sigma = 15\%$) and the populations at the two temperatures show nicely separated maxima (Figure 3B). It is in principle

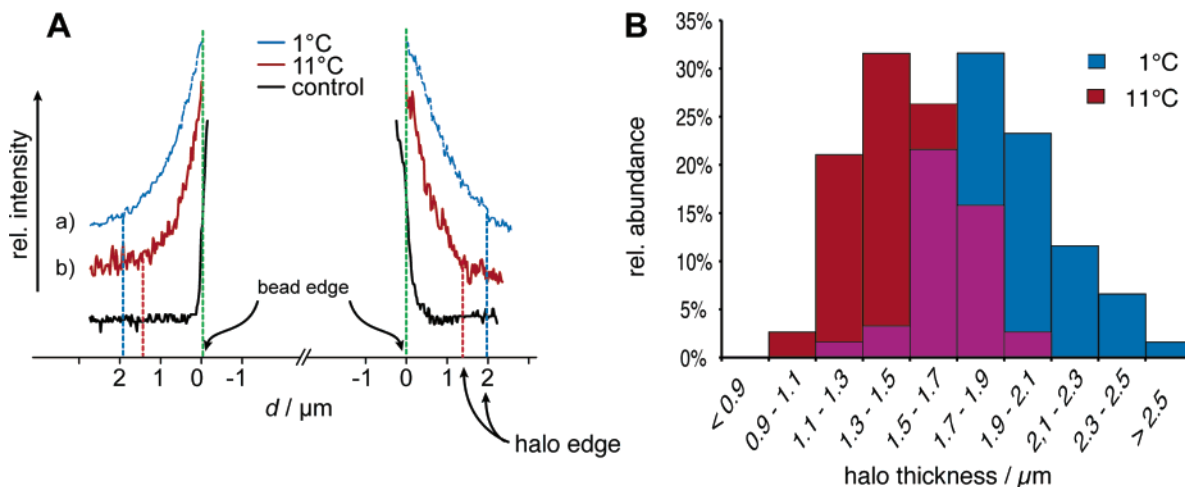


Figure 3. (A) Typical plot profiles from digital ESEM images. Intensity profiles (a and b) were taken along the dashed lines (a and b) in the unprocessed images (Figure 2). The control profile was taken from an untreated bead under the same conditions. Halo edges were defined at 10% relative intensity level where 100% was the intensity at the bead edge. Bead edges (green) and halo edges at 1 °C (blue) and at 11 °C (red) are marked with vertical dashed lines. (B) Thickness distribution of Tb^{3+} -labeled hyaluronan coats grafted on microspheres, as a function of temperature. The purple area denotes overlap. At 1 °C, the average coat thickness is 1.9 ± 0.3 μm ($N = 60$); at 11 °C the coat shrinks to 1.5 ± 0.2 μm ($N = 38$).

possible that only part of transition can be observed in the temperature–pressure window that is accessible experimentally. For example, further shrinkage might occur with increasing temperature above 11 °C. We note, however, that bulk hyaluronan in the presence of Gd^{3+} has a transition temperature of 2.5 °C (Figure 1). Beads prepared with Gd^{3+} instead of Tb^{3+} have reached their maximum shrinkage at 5 °C, and no further shrinkage occurs between 5 and 11 °C (data not shown). This indicates that the transitions on the beads are as sharp as in bulk and that on beads the total shrinkage (20%) is much less than in bulk (>90%). This is likely due to the covalent linking of the coat to the surface of the bead, which limits the mobility of the chains. Furthermore, we do not know how the transition is affected by the levels of Tb in the coat and how much of the Tb is lost during washing. We find the temperature-dependent shrinkage of the coats highly reproducible and conclude that, under the conditions described, the amounts of Tb are likely no longer affected by washing. The hyaluronan used here does not show the same reversibility in its volume transition that Prestwich and co-workers described (see above). This may be due to the higher molecular weight (2.4–3.6 vs 1.7 MDa) of the material or might reflect different concentrations of monovalent salt in the preparations. The hyaluronan on the beads has to go through this partially reversible transition once in the course of the preparation. It is thus possible that some of the reduced volume changes on the beads derive from general lack of reversibility. Nevertheless, the remaining effect is pronounced and occurs in the same well-defined temperature interval as the bulk transition.

Discussion

We have designed a procedure whereby hyaluronan coats of $> 1 \mu\text{m}$ thickness can be covalently grafted to polystyrene beads with no covalent modification of hyaluronan side chains. In fact, the only covalent modification is a number of bonds between the photolinker on the bead surface and the hyaluronan molecules closest to the bead surface. The procedure exploits the reverse temperature-dependent precipitation of lanthanide salts of hyaluronan. As part and parcel of the procedure, we have also imaged beads coated with Tb-labeled hyaluronan and have characterized the temperature-dependent variation in the coat thickness.

Grafting and Structure of the Coat. A key step to grafting thick coats on photo-cross-linker-modified polystyrene microspheres is the partially reversible coprecipitation of beads with hyaluronan from a relatively dilute hyaluronan solution upon the addition of TbCl_3 . This precipitation occurs rapidly at room temperature and can be partially reversed by cooling to 2–4 °C. Grafting under these conditions works where cross-linking from mere solutions of hyaluronan fails, because of the sharp decrease in volume of the hyaluronan phase. In essence, an infinite coordinative network of entangled hyaluronan chains with Tb^{3+} as inter- and intramolecular cross-linker is condensed on the surface of the beads (Scheme 2). In the process, the radius of gyration of individual chains is much decreased, bound water is set free, and the concentration of chains in the new phase is much higher than in the absence of Tb. As this network efficiently traps the reactive beads suspended in the solution, the reactive nitrene generated by irradiation has a much higher chance of reacting with hyaluronan chains rather than with solvent. Also, any given area on the bead can make contact

and thus link to more chains because of the reduced radius of gyration of each polymer chain.

It is reasonable to expect that after extensive washing only part of the chains in the coat are covalently bound to the surface, some chains possibly with more than one bond (Scheme 2). A layer of coiled hyaluronan grafted in multiple positions to the bead surface is not expected to reach a thickness greater than 200–400 nm, even when swollen. Thus the coat is composed of many layers. With increasing distance from the surface, the likelihood of a covalent bond between the bead and the hyaluronan chains drops. The chains that are not covalently attached to the bead are most likely bound to other chains by strong entanglement and coordinative cross-links mediated by Tb^{3+} . We know that Tb^{3+} remains bound in the coat because the coat can be imaged by ESEM and there is still a temperature response of the coat thickness (the latter will be discussed below). Tb^{3+} thus takes on the role that UO_2^{2+} took in previous imaging of hyaluronan coats around cells. Exactly how much Tb^{3+} is left is not, however, known. Any lanthanide cation can accommodate up to nine carboxylates, hydroxyl, or water ligands, while any hyaluronan chain can contribute thousands of carboxylates and hydroxyls. This multidentate multiligand binding is probably the reason for the high stability of the complex. The overall amount of hyaluronan–Tb complex grafted to the bead is still minute, as can be seen from the little residue left upon forced drying (Figure 2B).

Imaging by ESEM. It is thus water that makes up the bulk of the coat as imaged in ESEM. From 3D image reconstruction of fluorescently labeled cells, we know that the pericellular coat covers the entire surface of chondrocytes.⁷ From the similarity of the behavior of cells and beads under ESEM conditions, we conclude that a fully hydrated, three-dimensional gel coat covers the bead. Effectively, a bead is buried in a droplet of Tb–hyaluronan gel that is covalently linked to the surface of the bead. The shape of the gel droplet is affected by surface tension at the air–water interface and the contact angle of the hyaluronan gel to the underlying substrate. The boundary that we observe by ESEM is probably the lower limit, as in bulk water the surface tension does not confine the volume of the hyaluronan coat. Thus, there is no reason to assume that there is a sharp boundary at all. More likely, the concentration of hyaluronan falls to zero over a certain distance. The exact decay function is a very interesting physical property that could be investigated by photonic force microscopy (laser tweezers) rheology.²⁴

Temperature Response. We observe a reversible volume change of the grafted Tb–hyaluronan coat of about 20% (Figure 2C,D, Figure 3) The shrinkage with increasing T occurs in the same temperature interval (1–11 °C) as the corresponding bulk transition (Figure 1 and ref 18). However, the magnitude of the volume change is reduced.

The transition is likely an entropic effect. It is dependent on the nature of the cations, presence of monovalent salt, molecular weight of the hyaluronan, and temperature. Explanation of the effect on a molecular level within the classical framework of polymer²⁵ and polyelectrolyte theory²⁶ is difficult, because of the limitation of this effect to lanthanides and hyaluronan. Other

(24) Furst, E. M. *Soft Mater.* **2003**, *1*, 167–185.

(25) (a) de Gennes, P. *J. Phys.* **1976**, *37*, 1445–1452. (b) de Gennes, P. *Macromolecules* **1980**, *13*, 1069–1075. (c) Alexander, J. *J. Phys.* **1977**, *38*, 983–987.

polyelectrolytes, such as chondroitin sulfate, precipitate irreversibly when trivalent lanthanide cations are added.¹⁸ The salt dependence and the fact that small differences in the valence shell of lanthanides have a pronounced effect on the transition temperature (Figure 1 and ref 18) suggest that the overall transition behavior results from a subtle interplay between various factors. One obvious parameter is hydrogen-bond-dependent solvation of hyaluronan and its counterions in water, which tends to keep the network swollen and in solution. On the other hand, the high charge, high coordination numbers (up to 9), and largely entropic driving force of complex formation^{19,20} that are specific to lanthanide cations tend to cause aggregation and precipitation of the complexes. Another factor may be the hydrophobic solvation and aggregation behavior of the so-called hydrophobic patches formed by the C–H bonds on the top and bottom of the sugar rings.²⁷ While the LCST phase behavior of N-substituted acrylamides, where the hydrophobic effect plays a major role, is well understood,²¹ we are not able to offer a more detailed explanation of this highly specific phenomenon.

Our technique allows preparation of layers of biological proportions. However, at the structural level the coat is quite different from the pericellular coat on cells. Interestingly, pericellular coats labeled with Tb³⁺ were observed to shrink by 40–60% after the transition from 1 to 11 °C (manuscript in preparation). Thus, the transition with lanthanide salts occurs both on cells and on beads. It is known that the 5 μm thick coat of chondrocytes also comprises coordinatively cross-linking proteins such as aggrecan. The accepted model for hyaluronan–aggrecan interaction is the formation of bottle brush-type complexes where the keratan and chondroitin sulfate-decorated aggrecan chains radiate out from a stretched-out hyaluronan chain.²⁸ While it is well-known that the viscosity and elasticity of hyaluronan solutions dramatically increases upon addition of aggrecan,²⁹ it is important to point out that the hyaluronan chain interconnects aggrecan molecules and does so by weak

saccharide–protein complexes. Aggrecan does not in the chemical sense cross-link hyaluronan chains. The small number of polysaccharide chains these proteins can bind, their vastly larger dimensions, and comparatively weak protein–sugar interactions all differentiate them from the small, hard lanthanide ions with their high coordination numbers. In addition, hyaluronan molecules are likely grafted to the beads through multiple covalent bonds on beads, while they are generally thought to be attached at only one site to the cell surface. How these factors affect the formation of the pericellular coat in vivo and on microspheres will be the subject of future investigations.

Conclusions

We have demonstrated here a simple yet efficient exploit of the temperature-dependent phase transition of lanthanide–hyaluronan complexes for the preparation of covalently grafted, 1.5–2 μm thick layers of hyaluronan on polystyrene microspheres. This approach may also lend itself to the fabrication of soft polymer cushions for supported membranes¹³ or the generation of hyaluronan-functionalized surfaces with unique lubrication behavior.³⁰ Tb³⁺ was found to be a very good substitute for uranyl acetate as a contrast agent for ESEM imaging conditions. We further extended the use of wet-mode ESEM to imaging at different temperatures. This allowed observation of the temperature-dependent swelling behavior of Tb-labeled hyaluronan coats on microspheres. A relative shrinkage in thickness of ~20% between 1 and 11 °C was found. This is the first account of such a transition in a highly hydrated medium that could be observed directly by wet-mode ESEM.

Acknowledgment. D.J. is grateful for a postdoctoral fellowship from the Swiss Section of the Friends of the Weizmann Institute. This study was supported by the Clore Center for Biological Physics. L.A. is the incumbent of the Dorothy-and-Patrick-Gorman Professorial Chair of Biological Ultrastructure, and B.G. is an incumbent of the E. Neter Chair in Tumor and Cell Biology.

Supporting Information Available: Experimental details. This material is available free of charge via the Internet at <http://pubs.acs.org>.

JA0537474

- (26) (a) Tadmor, R.; Hernandez-Zapata, E.; Chen, N. H.; Pincus, P.; Israelachvili, J. N. *Macromolecules* **2002**, *35*, 2380–2388. (b) Dzubiella, J.; Moreira, A. G.; Pincus, P. A. *Macromolecules* **2003**, *36*, 1741–1752. (c) Pincus, P. *Macromolecules* **1991**, *24*, 2912–2919.
- (27) (a) Pratt, L. R. *Annu. Rev. Phys. Chem.* **2002**, *53*, 409–436. (b) Scheraga, H. A. *J. Biomol. Struct. Dyn.* **1998**, *16*, 447–460.
- (28) (a) Engel, J. *Methods Enzymol.* **1994**, *245*, 469–488. (b) Morgelin, M.; Heinegard, D.; Engel, J.; Paulsson, M. *Biophys. Chem.* **1994**, *50*, 113–128.
- (29) Meechai, N.; Jamieson, A. M.; Blackwell, J.; Carrino, D. A.; Bansal, R. J. *Rheol.* **2002**, *46*, 685–707.

- (30) (a) Benz, M.; Chen, N. H.; Israelachvili, J. J. *Biomed. Mater. Res., Part A* **2004**, *71A*, 6–15. (b) Tadmor, R.; Chen, N. H.; Israelachvili, J. *Macromolecules* **2003**, *36*, 9519–9526.